Supporting Information Available

High-Fidelity Fabrication of Au-Polymer Janus Nanoparticles using a Solution Template Approach

Tingling Rao[1], *Xuehui Dong*[1], *Bryan Katzenmeyer*[2], *Chrys Wesdemiotis*[1,2], *Stephen Z. D. Cheng*[1], *Matthew L. Becker*[1,3]*

[1]Department of Polymer Science, The University of Akron, Akron, OH 44325-3909

[2]Department of Chemistry, The University of Akron, Akron, OH 44325

[3]Center for Biomaterials in Medicine, Austen Bioinnovation Institute in Akron, Akron, OH, 44308

*To whom correspondence should be addressed, email: becker@uakron.edu

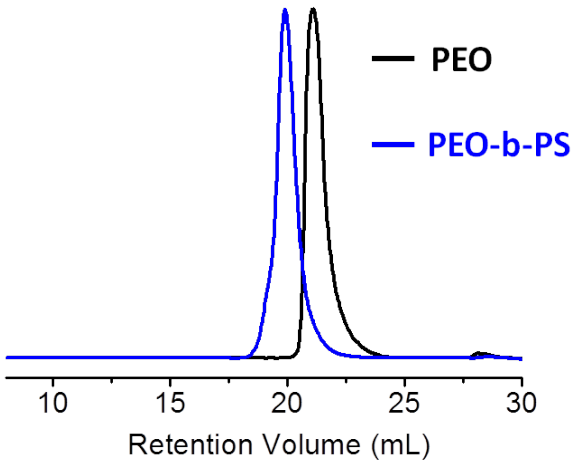

Figure S1. SEC curves of PEO precursor and PEO_{227}-b-PS_{442}.

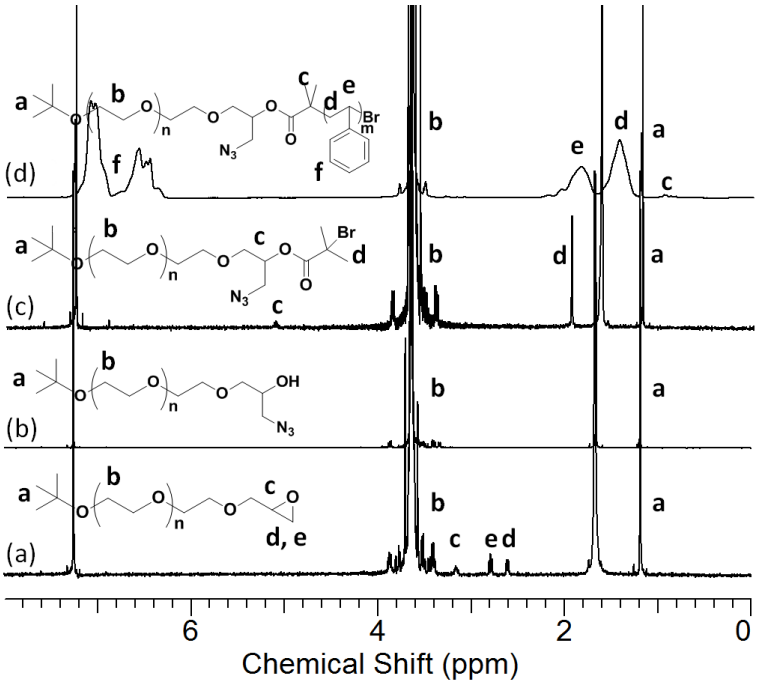

Figure S2. ^{1}H-NMR of PEO precursor and PEO_{227}-b-PS_{442}. The in-chain functional group N_3 can be used for extend the functionality, which now is under further investigation. (a) PEO-Epoxy: ($CDCl_3$, 500 MHz, ppm, δ): 3.64 (br, 900H, -C*H*$_2$C*H*$_2$O-), 3.16 (m, 1H, -C*H*(O)CH$_2$), 2.79 (m, 2H, -CH(O)C*H*$_2$), 2.61 (m, 1H, -CH(O)C*H*$_2$), 1.20 (s, 9H, (C*H*$_3$)$_3$C-O-). (b) PEO-(N_3)-OH: ^{1}H NMR ($CDCl_3$, 500 MHz, ppm, δ): 3.64 (br, 900H, -C*H*$_2$C*H*$_2$O-), 1.20 (s, 9H, (C*H*$_3$)$_3$C-O-). (c) PEO-(N_3)-Br: ^{1}H NMR ($CDCl_3$, 500 MHz, ppm, δ): 5.12 (m, 1H, -CH$_2$C*H*(CH$_2$N$_3$)OCO-), 3.64 (br, 900H, -C*H*$_2$C*H*$_2$O-), 1.93 (s, 6H, (-COC(C*H*$_3$)$_2$Br), 1.20 (s, 9H, (C*H*$_3$)$_3$C-O-). (d) ^{1}H NMR ($CDCl_3$, 500 MHz, ppm, δ): 6.30-7.40 (br, 2200H, -CH$_2$C*H*(-Ar)-), 3.64 (br, 900H, -C*H*$_2$C*H*$_2$O-), 1.67-2.15 (br, 440H, -CH$_2$C*H*(-Ar)-), 1.20-1.67 (br, 880H, -C*H*$_2$CH(-Ar)-), 1.20 (s, 9H, (C*H*$_3$)$_3$C-O-), 0.93 (m, 6H,-O-CO-C((C*H*$_3$)$_2$)CH$_2$-).

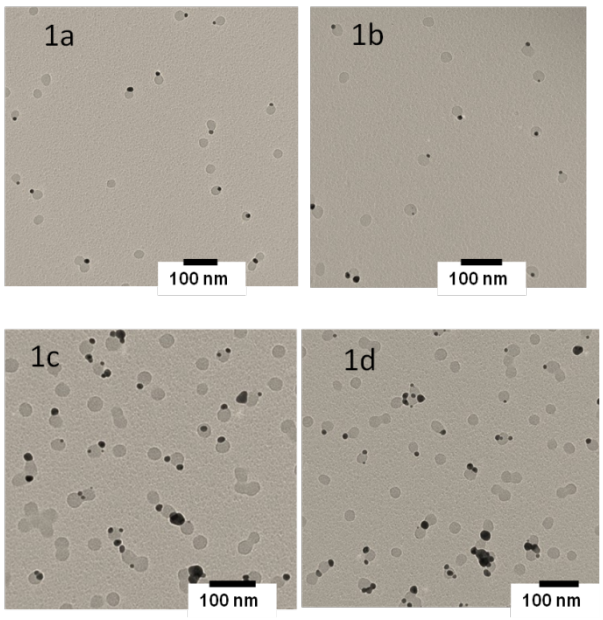

Figure S3. Representative TEM images from 1a to 1d. HEPES concentration was constant at 0.1 mol/L. Polymer concentration was gradually reduced from 1a to 1d, which were 1.4×10^{-6} mol/L, 1.0×10^{-6} mol/L, 6.0×10^{-7} mol/L and 2.0×10^{-7} mol/L, respectively. As polymer concentration decreases, the overall portion of Janus nanoparticle is decreasing and the capability to control Au nanoparticles is also impaired. Au nanoparticle aggregates and blank micelles were not counted for the histograms.

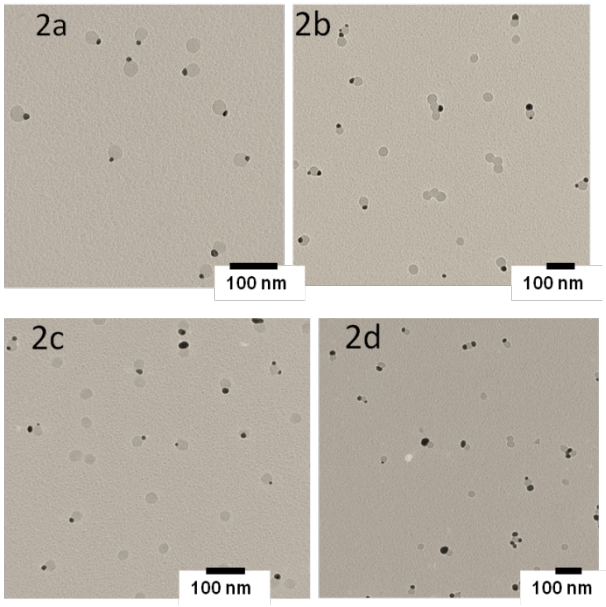

Figure S4. Representative TEM images from 2a to 2d.. HEPES concentration was constant at 0.3 mol/L. Polymer concentration was gradually reduced from 2a to 2d, which were 1.4×10^{-6} mol/L, 1.0×10^{-6} mol/L, 6.0×10^{-7} mol/L and 2.0×10^{-7} mol/L, respectively. The overall portion of Janus particles is decreasing as polymer concentration decreased, but the system still maintains the ability to morphology of Au nanoparticles

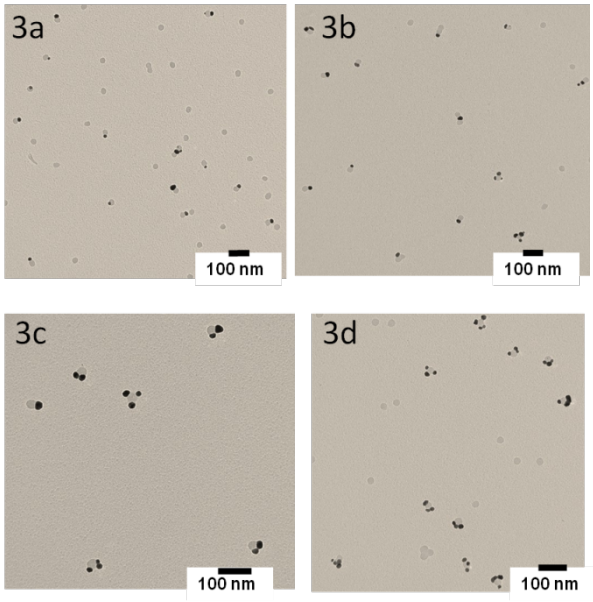

Figure S5. Representative TEM images from 3a to 3d. HEPES concentration was constant at 0.5 mol/L. Polymer concentration was gradually reduced from 3a to 3d, which were 5.6×10^{-7} mol/L, 4.0×10^{-7} mol/L, 2.4×10^{-8} mol/L and 8.0×10^{-8} mol/L, respectively. The overall portion of Janus nanoparticle is reduced and the destruction of gold nanoparticle/micelle ratio for each hybrid entity is shifting to a higher value as polymer concentration decreases.

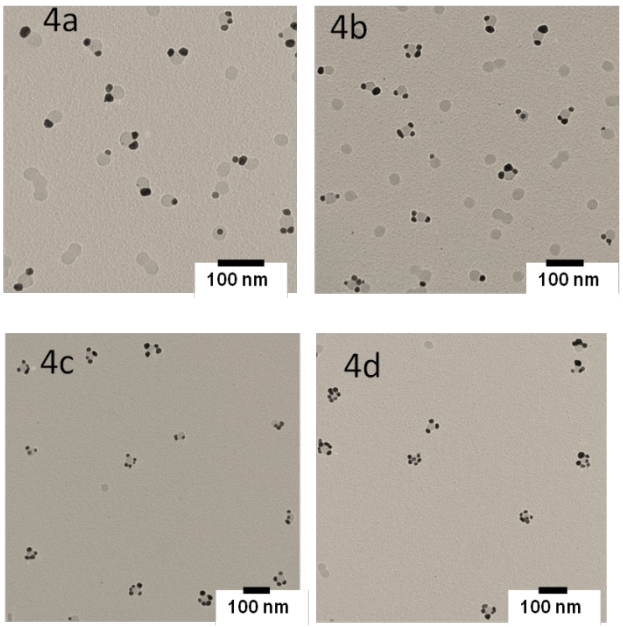

Figure S6. Representative TEM images from 4a to 4d. The HEPES concentration was constant at 0.7 mol/L. Polymer concentration was gradually reduced from 4a to 4d, which were 5.6×10^{-7} mol/L, 4.0×10^{-7} mol/L2.4×10^{-8} mol/L and 8.0×10^{-8} mol/L, respectively. The overall portion of Janus nanoparticle is further reduced and the destruction of gold nanoparticle/micelle ratio for each hybrid entity is shifting to a even higher value as polymer concentration decreases.

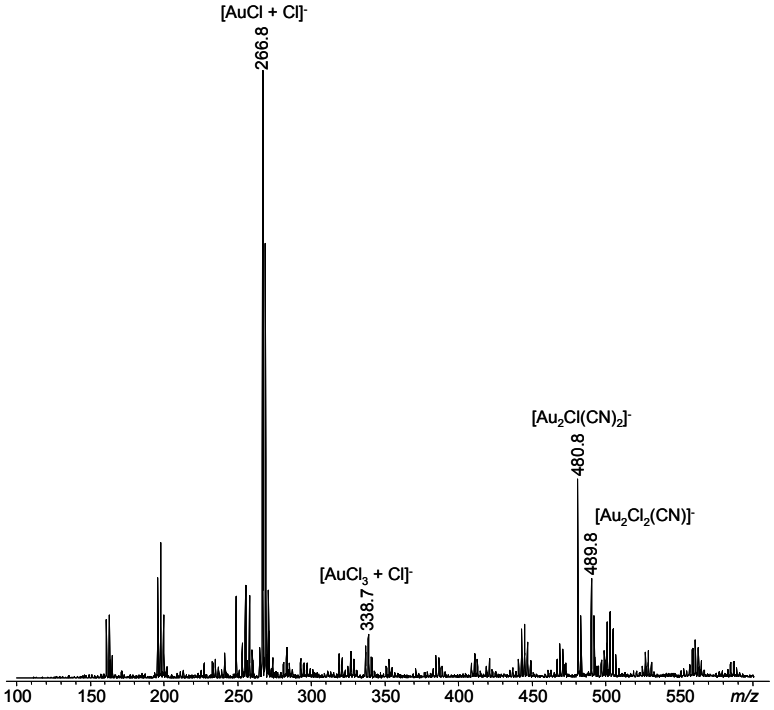

Figure S7. ESI-MS spectrum of the master solution (0.7 mM $HAuCl_4$ in water). All gold-containing ions are labeled. See Table S1 for ion intensities.

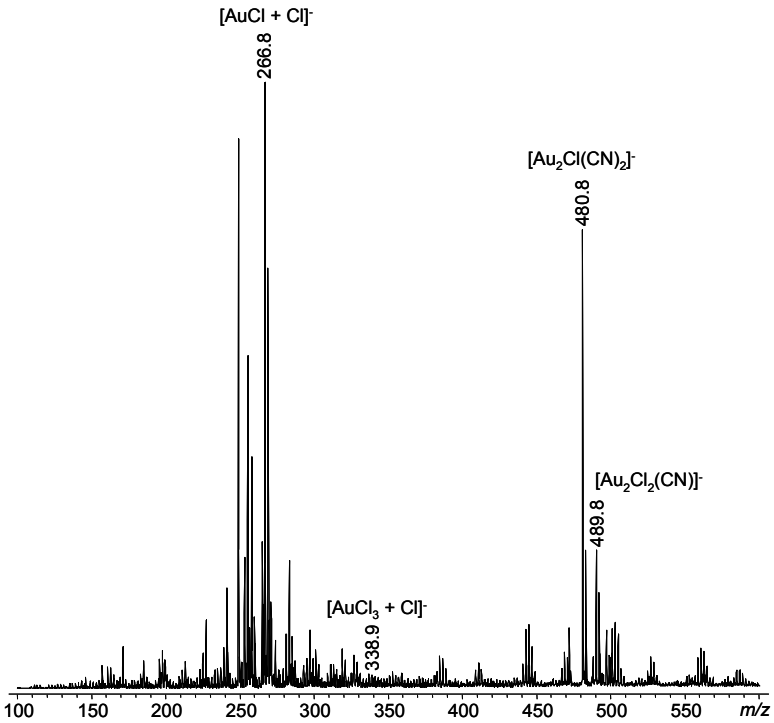

Figure S8. ESI-MS spectrum after the addition of micelles to the master solution. All gold-containing ions are labeled. See Table S1 for ion intensities.

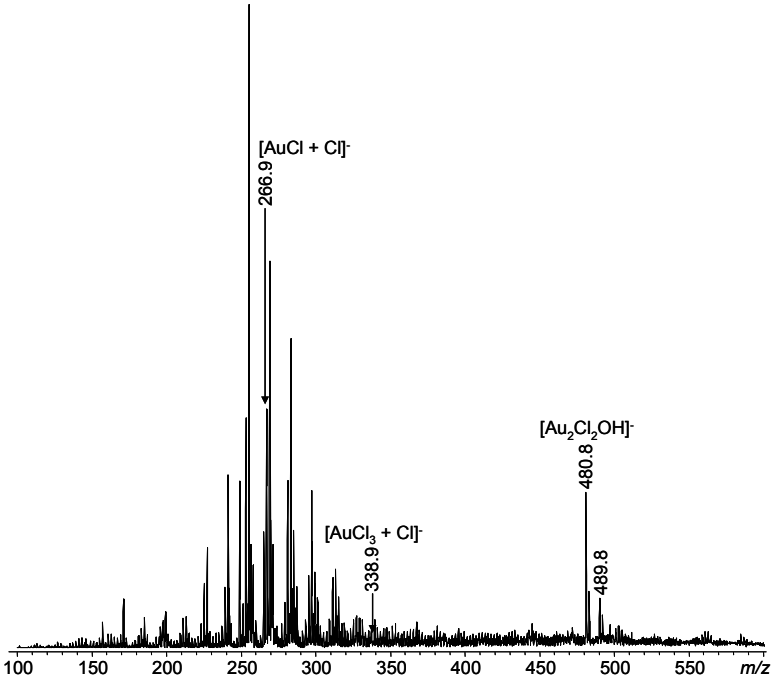

Figure S9. ESI-MS spectrum after centrifuging to remove micelles. All gold-containing ions are labeled. See Table S1 for ion intensities.

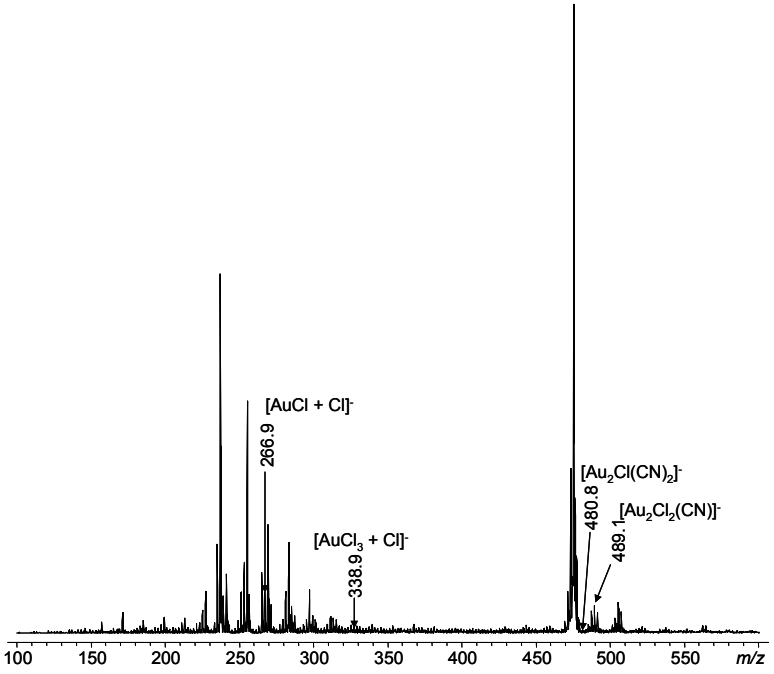

Figure S10. ESI-MS spectrum after reducing $HAuCl_4$ to Au and centrifuging to remove Au and micelles. All gold-containing ions are labeled. See Table S1 for ion intensities.

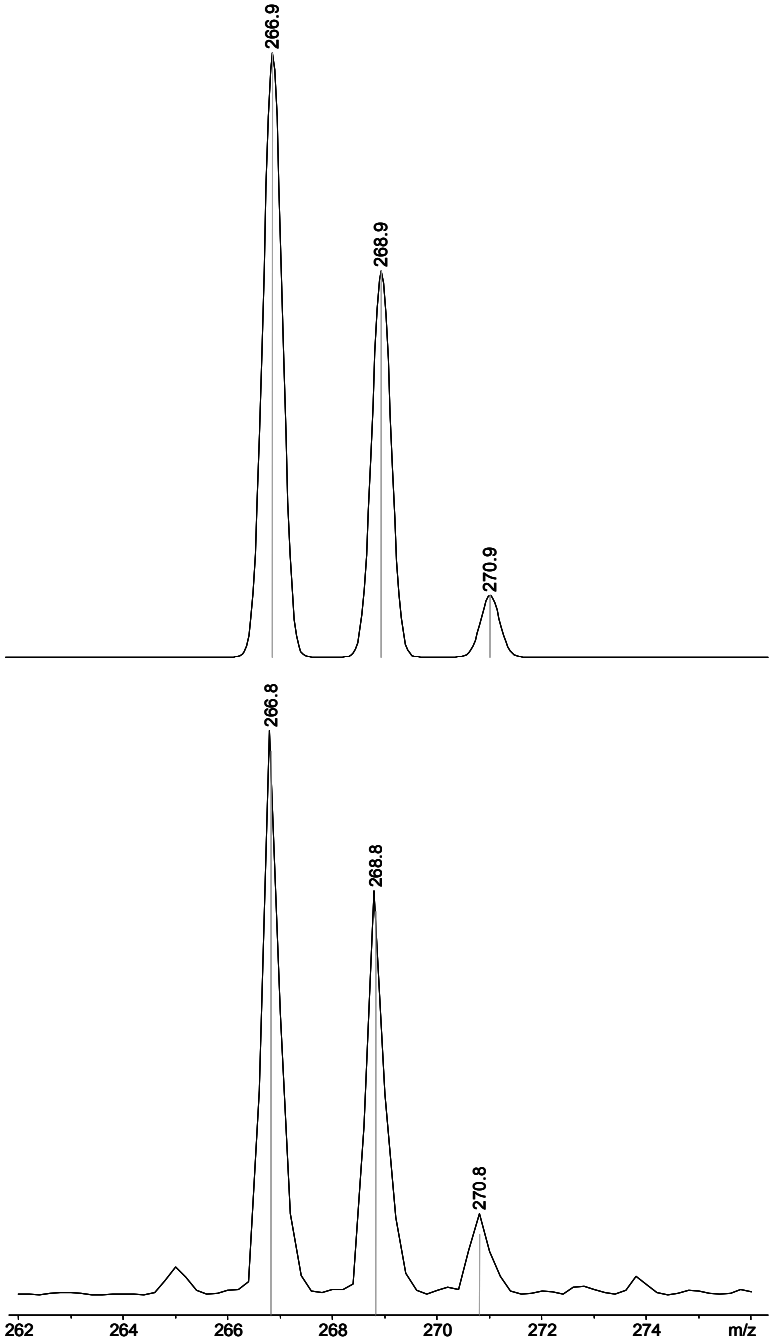

Figure S11. ESI-MS spectra of experimental (bottom) and theoretical (top) of $[AuCl + Cl]^-$ (*m/z* 266).

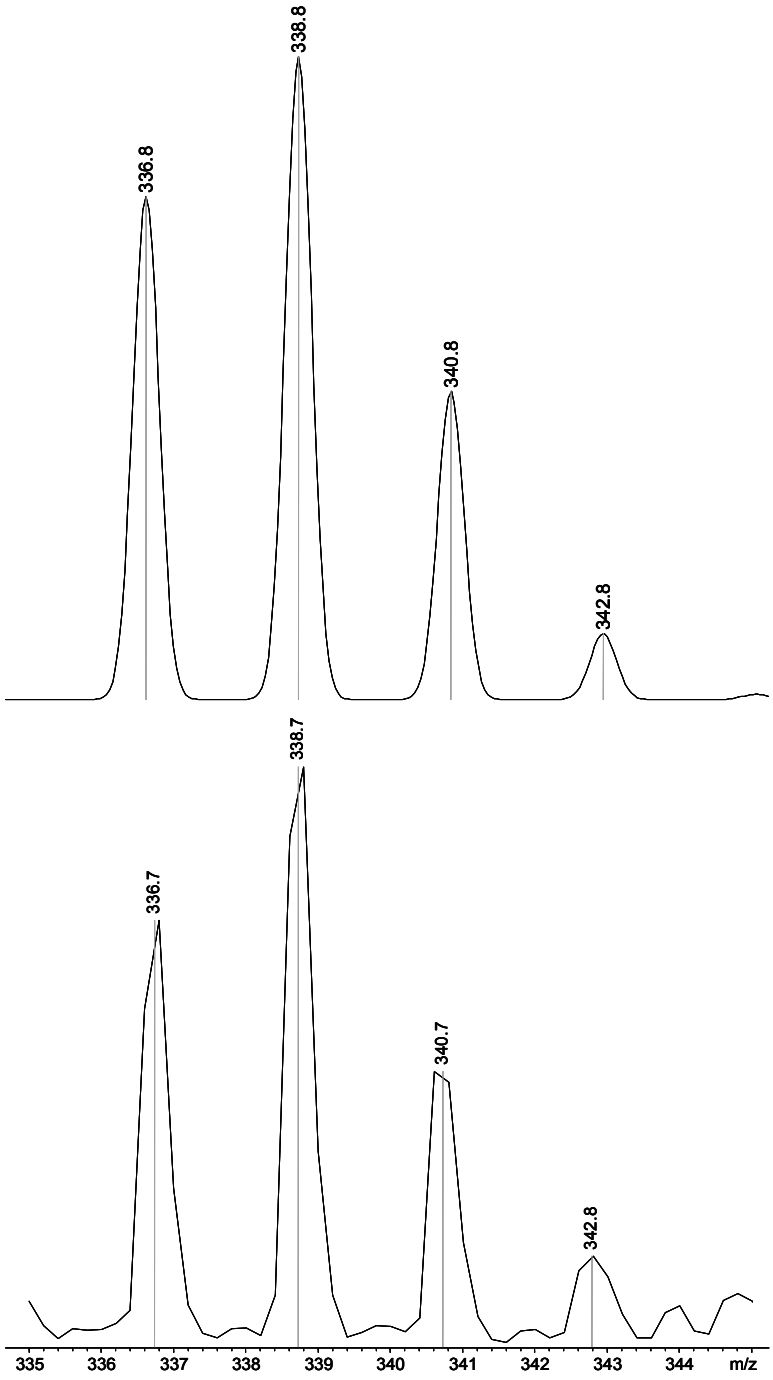

Figure S12. ESI-MS spectra of experimental (bottom) and theoretical (top) of $[AuCl_3 + Cl]^-$ (*m/z* 338).

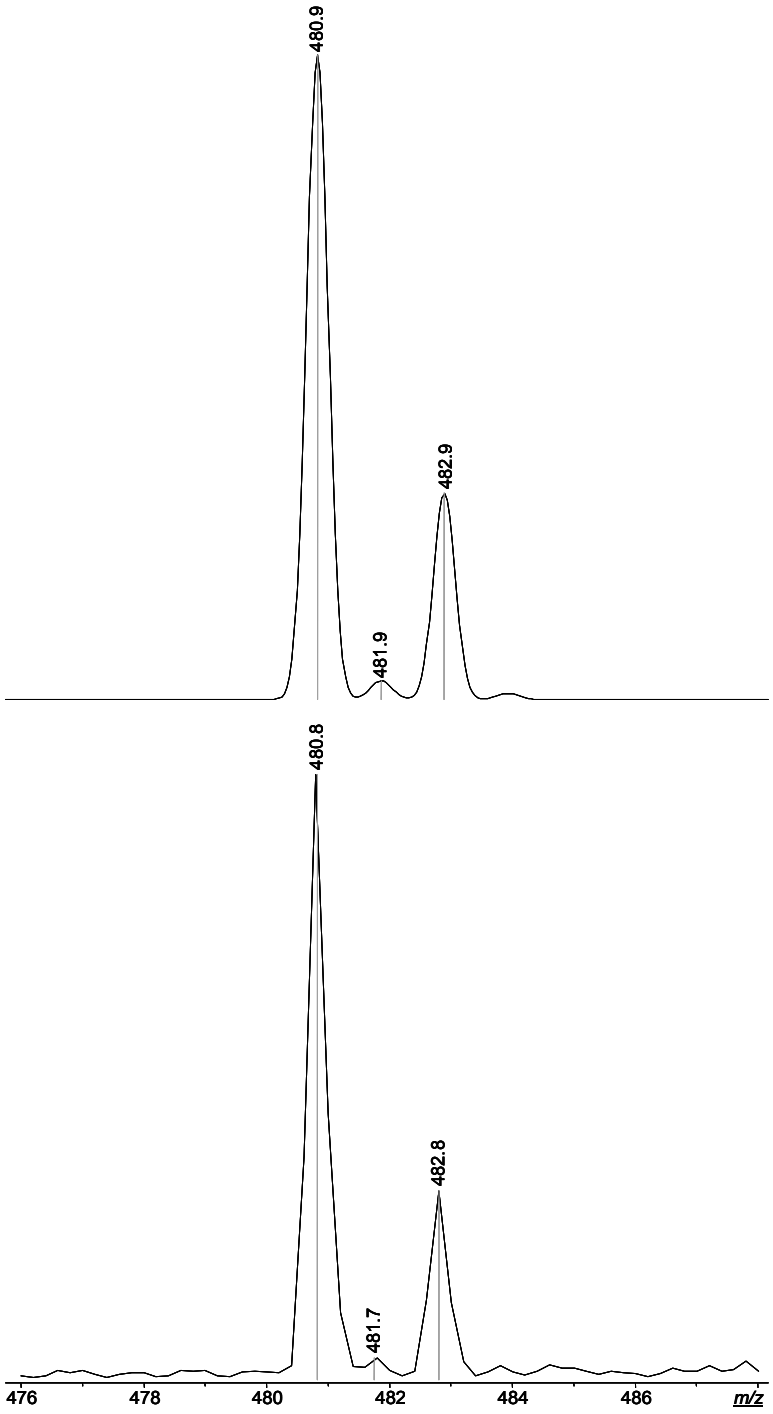

Figure S13. ESI-MS spectra of experimental (bottom) and theoretical (top) of $[Au_2Cl(CN)_2]^-$ (*m/z* 481).

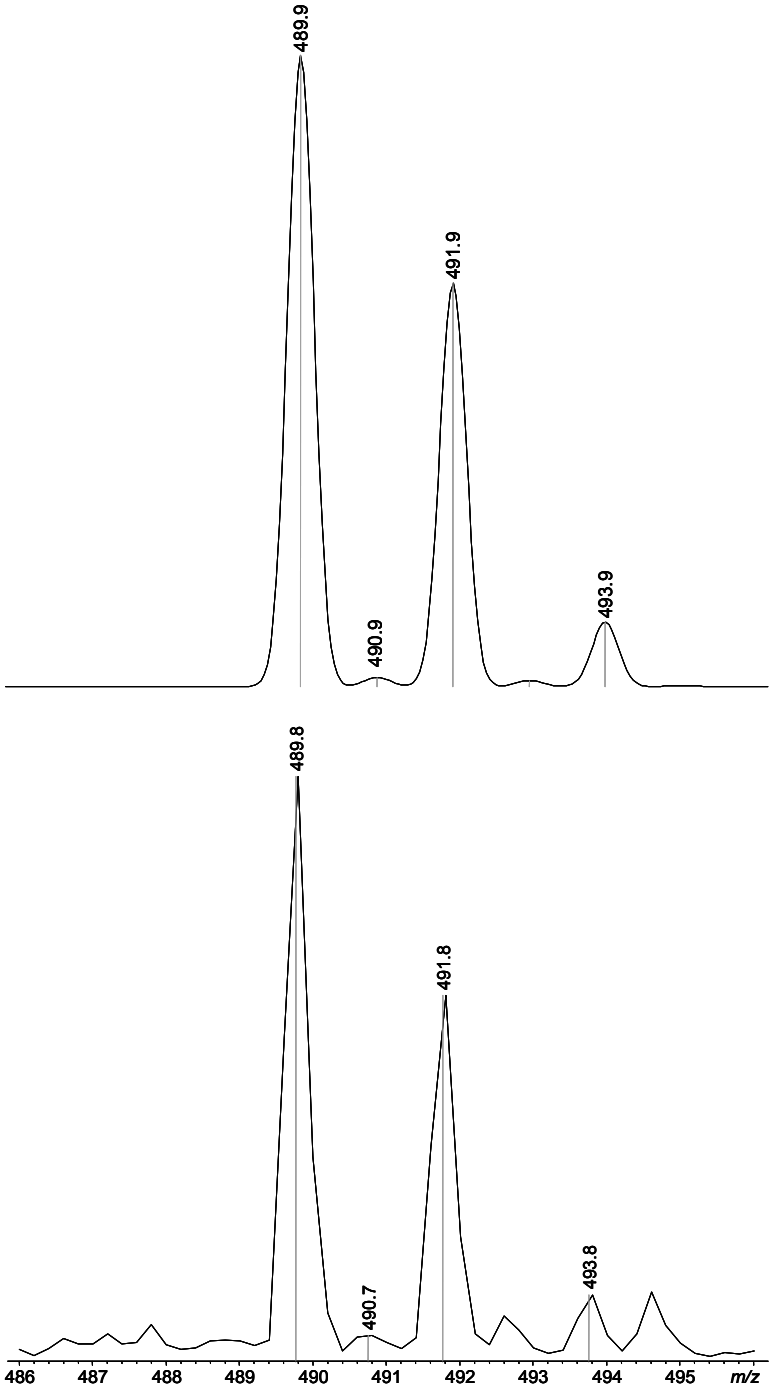

Figure S14. ESI-MS spectra of experimental (bottom) and theoretical (top) of $[Au_2Cl_2(CN)]^-$ (*m/z* 490).

Table S1

Solution	$HAuCl_4$ (master)	$HAuCl_4$ + Micelle	Supernatant	**Reduced to Au**
m/z 266.9 Intensity	352523	110601	58984	4930
m/z 338.8 Intensity	25440	2454	1651	1131
m/z 480.9 Intensity	115411	83794	38553	1253
m/z 489.9 Intensity	57589	25244	12120	11014

m/z 266.8, $[AuCl + Cl]^-$

m/z 338.7, $[AuCl_3 + Cl]^-$

m/z 480.8, $Au_2Cl(CN)_2]^-$

m/z 489.9, $[Au_2Cl_2(CN)]^-$